Electronic Supplementary Information (ESI) for

Substrate selectivity and its mechanistic insight of the photo-responsive non-nucleoside triphosphate for myosin and kinesin

Md. Jahirul Islam[1,2,†], Kazuya Matsuo[1,2,†], Halley M. Menezes[1,2], Masayuki Takahashi[3], Hidehiko Nakagawa[4], Akira Kakugo[3], Kazuki Sada[3] and Nobuyuki Tamaoki[1,2,*]

1. Research Institute for Electronic Science, Hokkaido University, Kita 20, Nishi 10, Kita-Ku, Sapporo, Japan

2. Graduate School of Life Science, Hokkaido University, Kita 10, Nishi 8, Kita-ku, Sapporo, Japan

3. Faculty of Science, Hokkaido University, Kita 10, Nishi 8, Kita-ku, Sapporo, Japan

4. Graduate School of Pharmaceutical Sciences, Nagoya City University, 3-1, Tanabe-dori, Mizuho-ku, Nagoya, Japan

† These authors contributed equally to this work.

* Correspondence and requests for materials should be addressed to N. T. (E-mail: tamaoki@es.hokudai.ac.jp).

Table of Contents

1. Reverse-phase (RP) HPLC profile of 1c

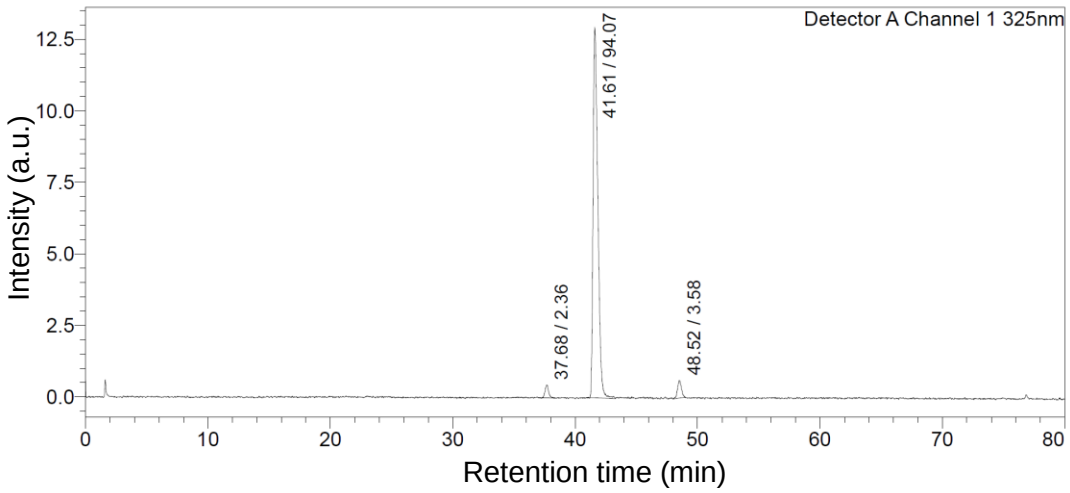

Fig. S1 RP HPLC chromatogram of **1c.** Retention time: 41.61 min (94%), Column: Mightysil, RP-18 GP (L) 150-4.6 (5µm) (Kanto Chemical). Eluent: 10–70 % of CH_3CN in sodium phosphate buffer (pH 6) for 80 min. Monitoring wavelength: 325 nm. Flow rate: 1.0 mL / min at room temperature.

2. UV-VIS absorption spectra of 1b–1d at different light irradiation condition

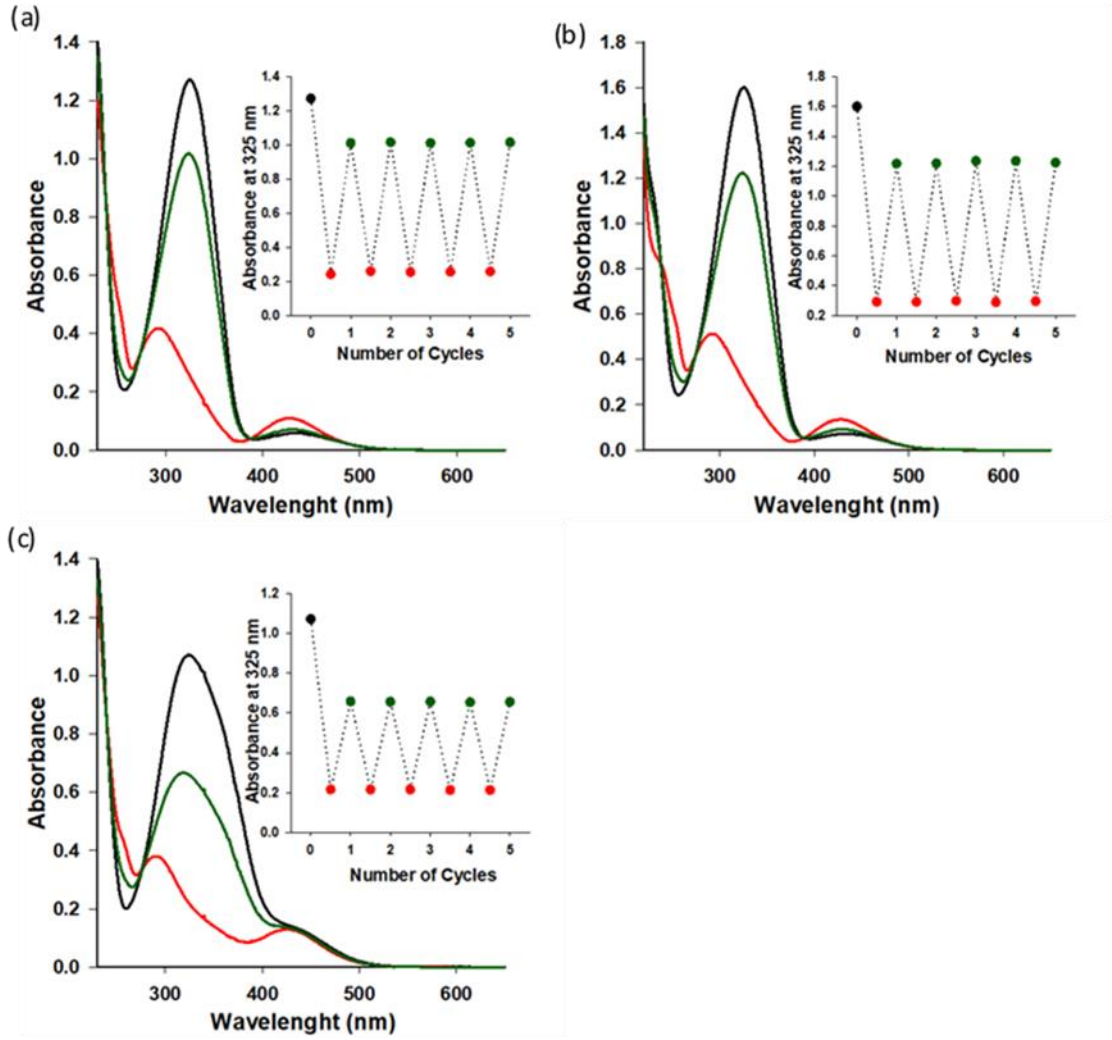

Fig. S2 UV-VIS absorption spectra of **1b** – **1d** at before irradiation (BI) condition, UV photo stationary state (PSS), and VIS PSS. UV-VIS absorption spectra of (a) **1b** (8.9×10^{-4} M), (b) **1c** (9.5×10^{-4} M), (c) **1d** (7.1×10^{-4} M) in BRB-80 buffer at 25 °C. BI (black line), UV PSS (red line), VIS PSS (dark green line). Insets: Absorbance changes after the alternate irradiations with UV (20 sec) and VIS (150 sec) light for 5 cycles.

3. *cis*-to-*trans* isomer ratio of AzoTP derivatives at the UV and VIS PSS

Table S1. Ratio of *cis* and *trans* isomers at the UV and VIS PSS

AzoTP derivatives	UV PSS		VIS PSS	
	cis (%)	*trans* (%)	*cis* (%)	*trans* (%)
1a	92	8	38	62
1b	87	13	25	75
1c	88	12	26	74
1d	93	7	50	50
1e	93	7	35	65

We determined the *cis*-to-*trans* isomer ratio of **1a**, **1b**, **1d**, and **1e** using ^{1}H NMR spectroscopy previously.[1,2]

Estimation of *cis*-to-*trans* ratio of **1c** at UV and VIS PSS:

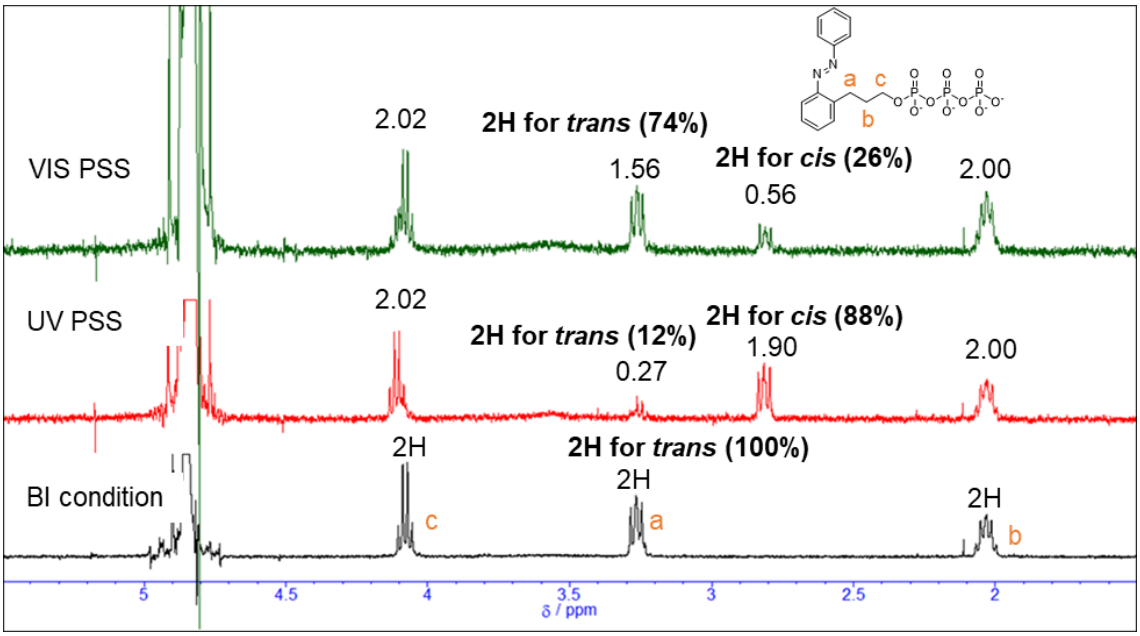

Fig. S3 ^{1}H NMR spectra of **1c** in D_2O prior to irradiation and after irradiation with the UV and VIS light (at PSS condition). The area for methylene protons of **1c** at 3.27 ppm was studied at before irradiation (BI) condition; after irradiation with UV (PSS); and after irradiation with VIS (PSS). At UV PSS, *cis* to *trans* ratio was 88 : 12 and at VIS PSS, *cis* to *trans* ratio was 26 : 74.

4. Thermal stability of *cis* isomer of compound 1a–1e

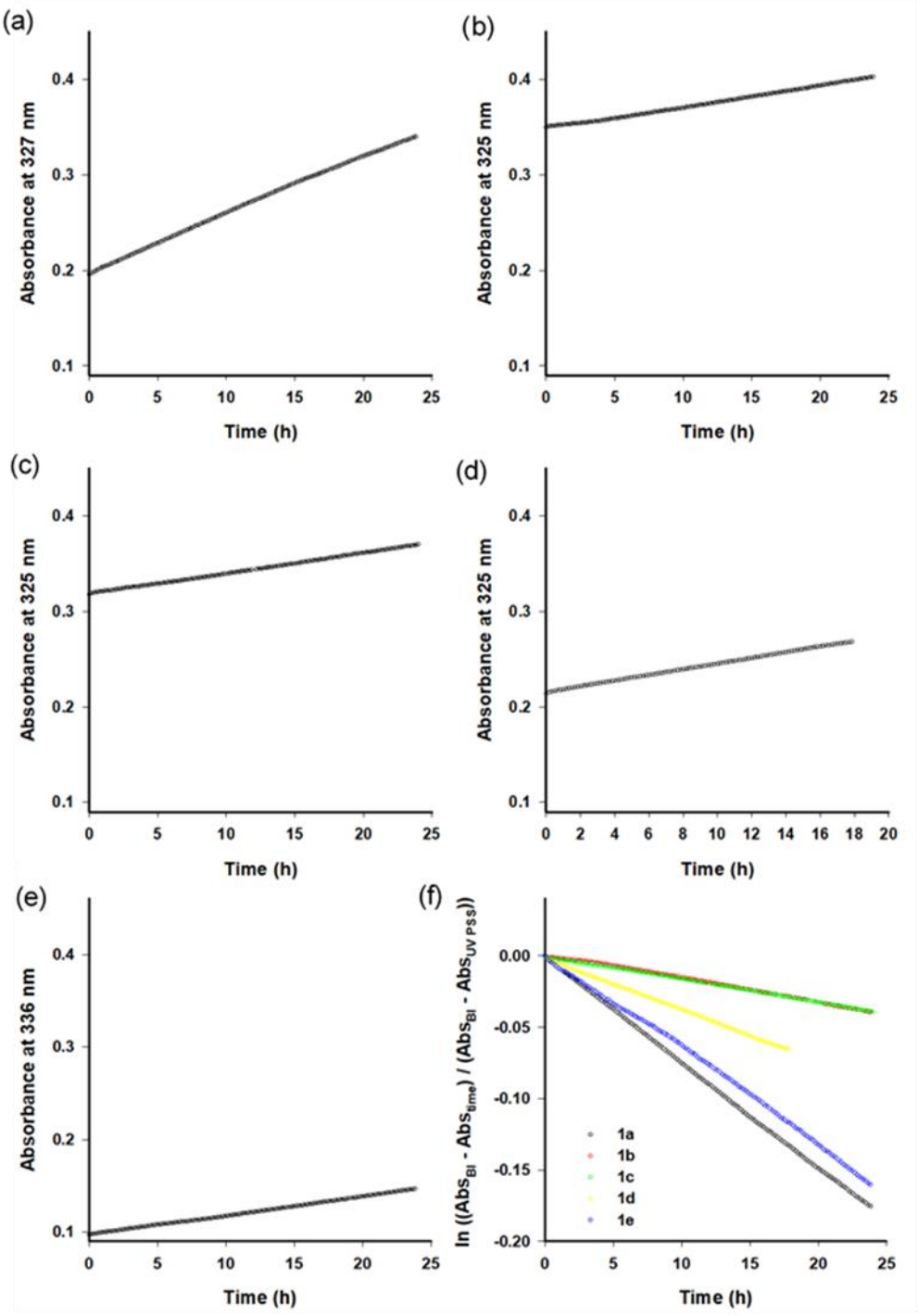

Fig. S4 Time course of the absorbance of (a) **1a** at 327 nm, (b) **1b** at 325 nm, (c) **1c** at 325 nm, (d) **1d** at 325 nm, (e) **1e** at 336 nm in BRB-80 buffer (pH 6.9) after UV irradiation and then incubated under dark condition at 25 °C. Conditions: [**1a**] = 6.8×10^{-4} M, [**1b**] = 12.1×10^{-4} M, [**1c**] = 10.0×10^{-4} M, [**1d**] = 7.1×10^{-4} M, [**1e**] = 3.0×10^{-4} M. (f) The plot for thermal isomerization rate determination of **1a-1e** under dark condition at 25 °C; equation, $\ln\left(\frac{Abs\ (\mathrm{BI}) - Abs\ (\mathrm{time})}{Abs\ (\mathrm{BI}) - Abs\ (\mathrm{UV\ PSS})}\right) = -kt$ was used to determine the rate of the thermal isomerization reaction where *Abs* (BI), Absorbance at before irradiation; *Abs* (UV PSS), Absorbance at UV photo stationary state; *Abs* (time), Absorbance at different time interval in dark start from UV PSS. Rate constants, k = 0.0074 h^{-1} ($t_{1/2}$ = 94 h) for **1a**, k = 0.0016 h^{-1} ($t_{1/2}$ = 4.3 $\times$ 10^2 h) for **1b**, k = 0.0016 h^{-1} ($t_{1/2}$ = 4.3 × 10^2 h) for **1c**, k = 0.0037 h^{-1} ($t_{1/2}$ = 1.9 × 10^2 h) for **1d**, k = 0.0066 h^{-1} ($t_{1/2}$ = 1.1 × 10^2 h) for **1e**.

5. AzoTPs (1a, 1b, 1d and 1e) in actin-myosin system as photoresponsive energy molecules

Table S2. Summary of AzoTP derivatives (**1a**, **1b**, **1d** and **1e**) in actin-myosin system

AzoTP derivatives/ATP	V_{max} (μm/s)	K_m (mM)	Gliding velocity switching* (%)
1a[2]	1.5 ± 0.04	0.10 ± 0.01	54
1b[2]	1.0 ± 0.1	0.18 ± 0.04	80
1d[2]	1.9 ± 0.2	0.091 ± 0.02	79
1e[2]	1.7 ± 0.2	0.27 ± 0.09	81

*Gliding velocity switching between *trans* and *cis*-rich state of AzoTP derivatives at saturated concentration, 1.0 mM for **1a** and **1e**; 0.50 mM for **1b** and **1d**.

6. Myosin-based actin filament gliding velocity depending on the concentration of triphosphate energy molecules

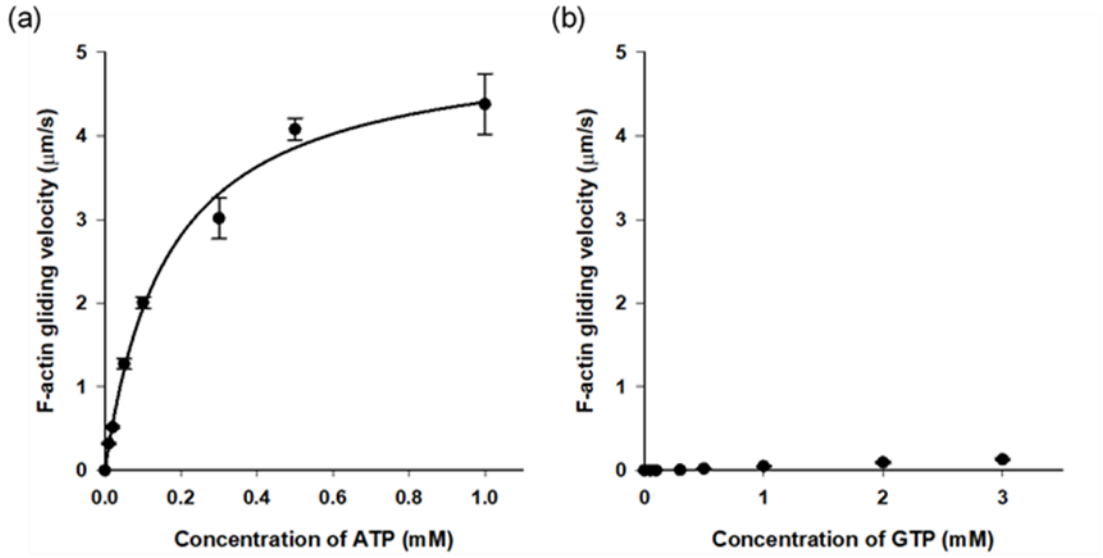

Fig. S5 Actin filament gliding motility with triphosphate energy molecule. (a) Gliding velocity depending on the concentration of ATP. (b) Gliding velocity with respect to the concentration of GTP. Solid black line: curve fitting using the Michaelis-Menten equation (K_m = 0.16 ± 0.02 mM, V_{max} = 5.1 ± 0.2 μm/sec for ATP). These K_m and V_{max} values with ATP were different from our formal report[2] because we used the different batch of myosin and actin from our previous report in this new experiment. Error bars represent the standard deviation of 10 actin filaments in a single flow cell.

7. Kinesin-based microtubule gliding velocity depending on the concentration of triphosphate energy molecules

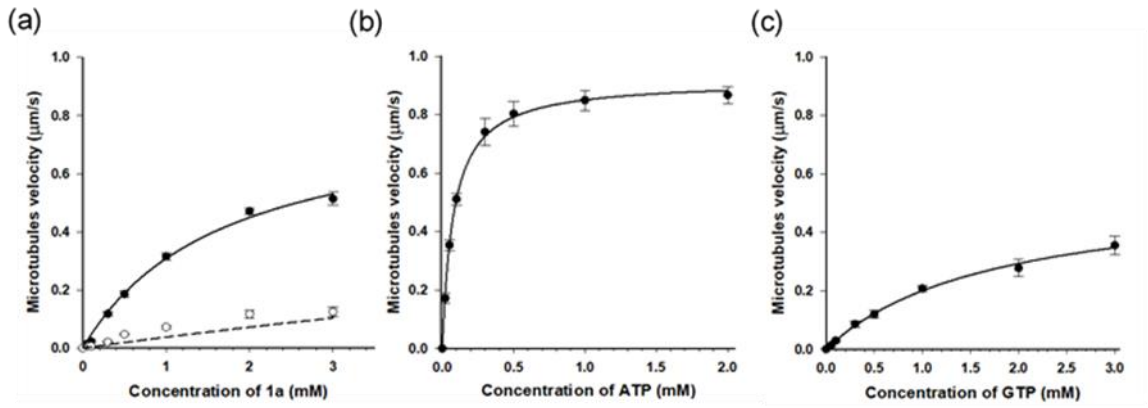

Fig. S6 Kinesin-based microtubule gliding velocity depending on the concentration of triphosphate energy molecules (filled circle (●): before irradiation and open circle (○): UV irradiation). Gliding velocity with respect to the concentration of (a) **1a**, (b) ATP, and (c) GTP. Solid black line: curve fitting using the Michaelis-Menten equation (K_m = 1.7 ± 0.2 mM, V_{max} = 0.83 ± 0.06 μm/sec for **1a**; K_m = 0.079 ± 0.003 mM, V_{max} = 0.92 ± 0.01 μm/sec for ATP, and, K_m = 1.8 ± 0.2 mM, V_{max} = 0.55 ± 0.03 μm/sec for GTP). Dash black line: theoretical curve derived from solid black line for remaining *trans* isomer (8%) in *cis* rich state of **1a**. Error bars represent the standard deviation of 10 microtubules in a single flow cell.

8. Reversible photoregulation of the microtubule gliding velocity with AzoTP derivatives

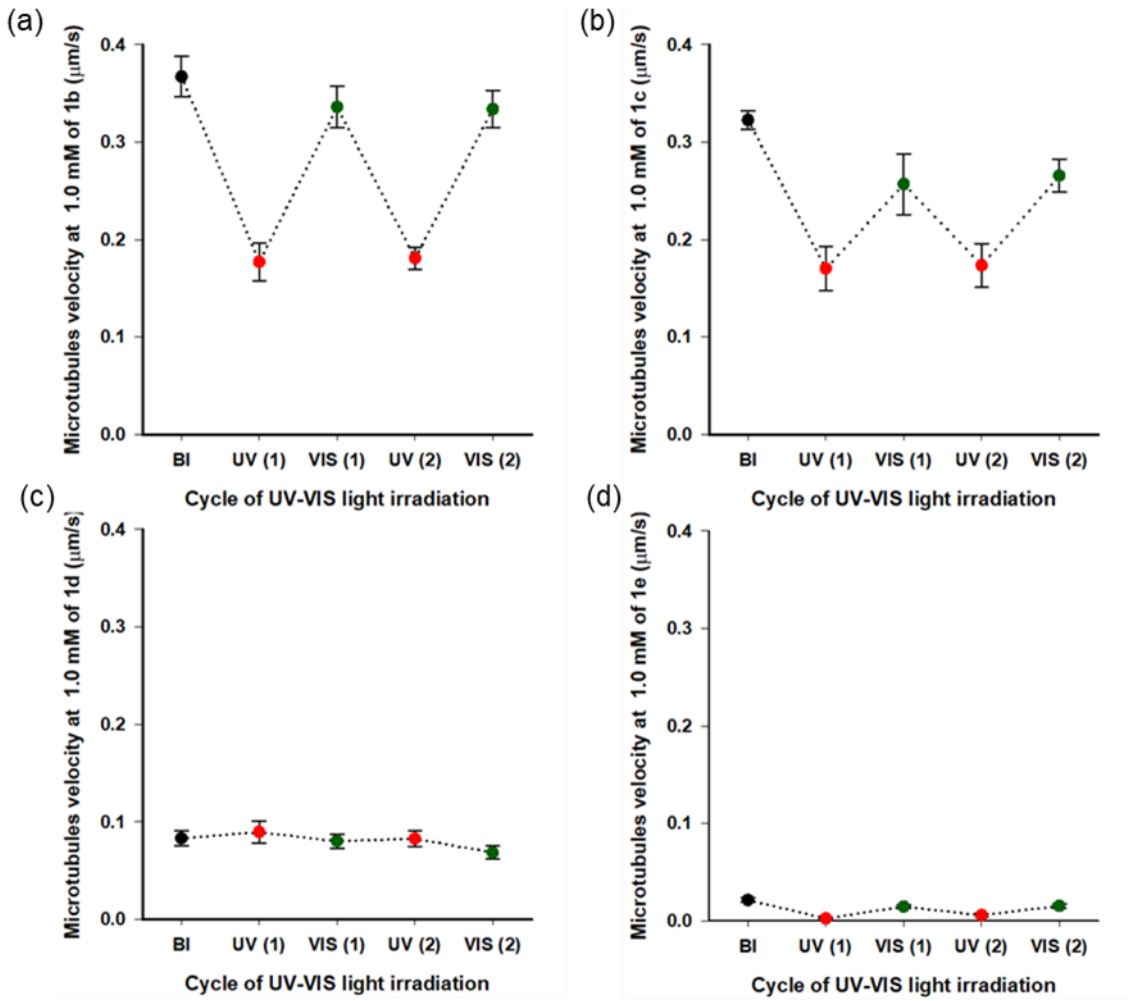

Fig. S7 Reversible photoregulation of the microtubule gliding velocity induced by AzoTP derivatives. (BI: before irradiation; UV: after irradiation with 365 nm light; Vis: after irradiation with 436 nm light). (a) **1b**, (b) **1c**, (c) **1d** and (d) **1e**. Error bars represent the standard deviation of 10 microtubules in a single flow cell.

9. Binding mode of ATP in kinesin-1 and myosin II motor domain

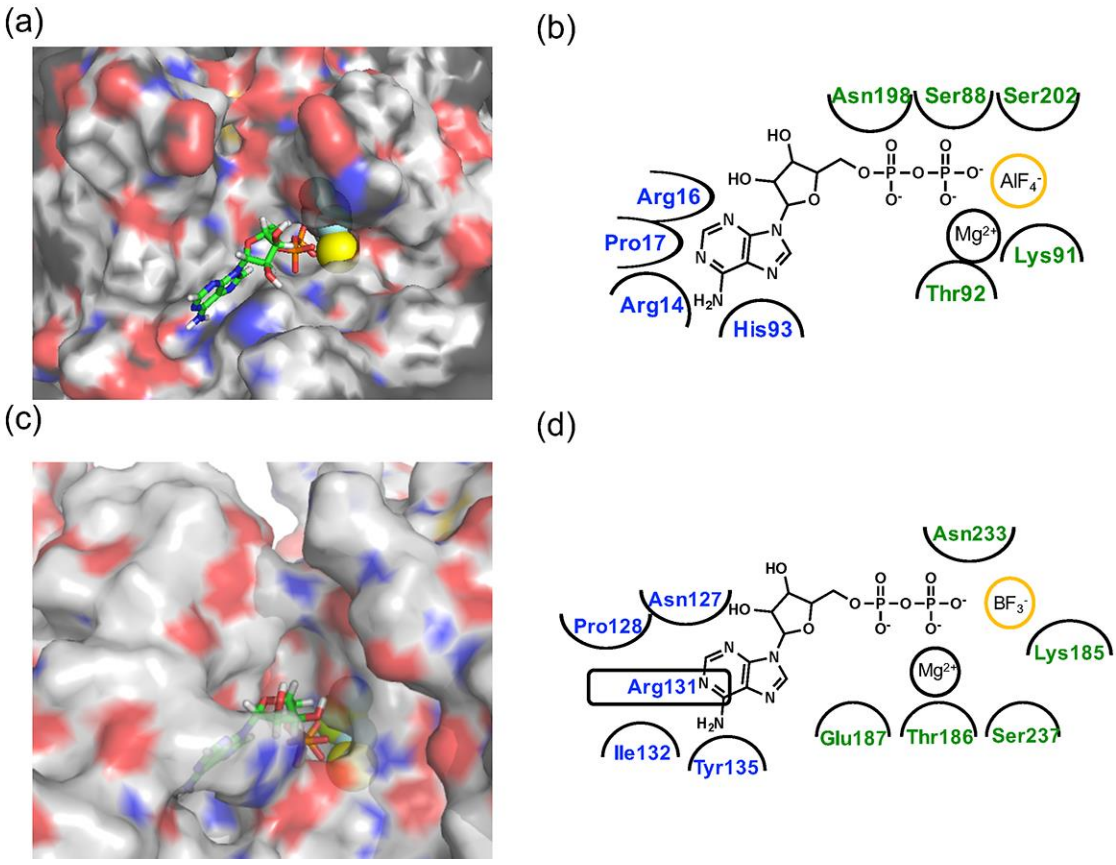

Fig. S8 X-ray crystallography analyses of ATP analogues with kinesin-1 and myosin II motor domain. X-ray crystal structures obtained from RCSB Protein Data Bank (PDB entry code: 4HNA for kinesin-1 and 1MMD for myosin II) were used. All figures of simulated results were created with pymol (DeLano Scientific). (a) X-ray structure and (b) binding modes of ADP-Mg-AlFx in kinesin-1. (c) X-ray structure and (d) binding modes of ADP-Mg-BFx in myosin II. In X-ray structures, ADP were represented by a stick mode. Magnesium ion (yellow) and BF_3^- or AlF_4^- was done by a ball mode. In the figures of binding modes, the amino acid resides composing ARBS were colored in blue and the residues composing the triphosphate binding site were colored in green.

10. Information of Supplementary Movies

Movie S1: Movie (total 8 min, 10 fps) in kinesin-myosin composite motility assay using **1e** (1.0 mM). *In situ* photoregulation of microtubules and actin filaments motility was studied by irradiating alternatingly with UV (365nm) and VIS (436 nm) light. AzoTP **1e** could drive actin filaments with photoreversibility (BI : 1.1 ± 0.04 μm/sec, UV : 0.27 ± 0.01 μm/sec and VIS : 0.88 ± 0.03 μm/sec at 1.0 mM), whereas it could not drive microtubules efficiently (BI : 0.054 ± 0.01 μm/sec UV : 0.014 ± 0.003 μm/sec and VIS : 0.040 ± 0.01 μm/sec at 1.0 mM).

Movie S2: Movie (total 4 min, 10 fps) in kinesin-myosin composite motility assay using ATP (0.20 mM). ATP could drive both of actin filaments and microtubules efficiently (3.3 ± 0.3 μm/sec for actin filaments and 0.71 ± 0.02 μm/sec for microtubules).

11. NMR Spectral data

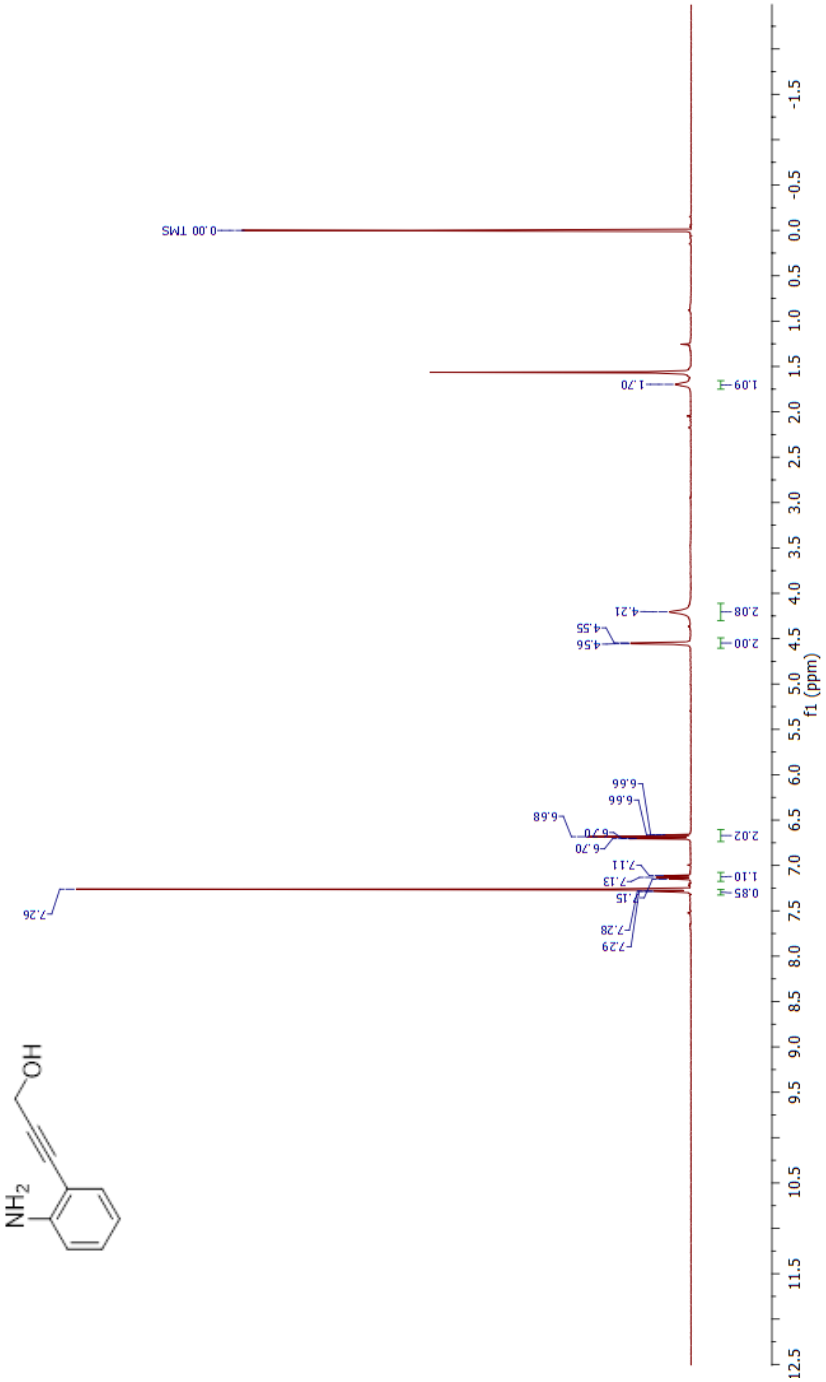

Fig. S9 ^{1}H NMR of **1c**-1

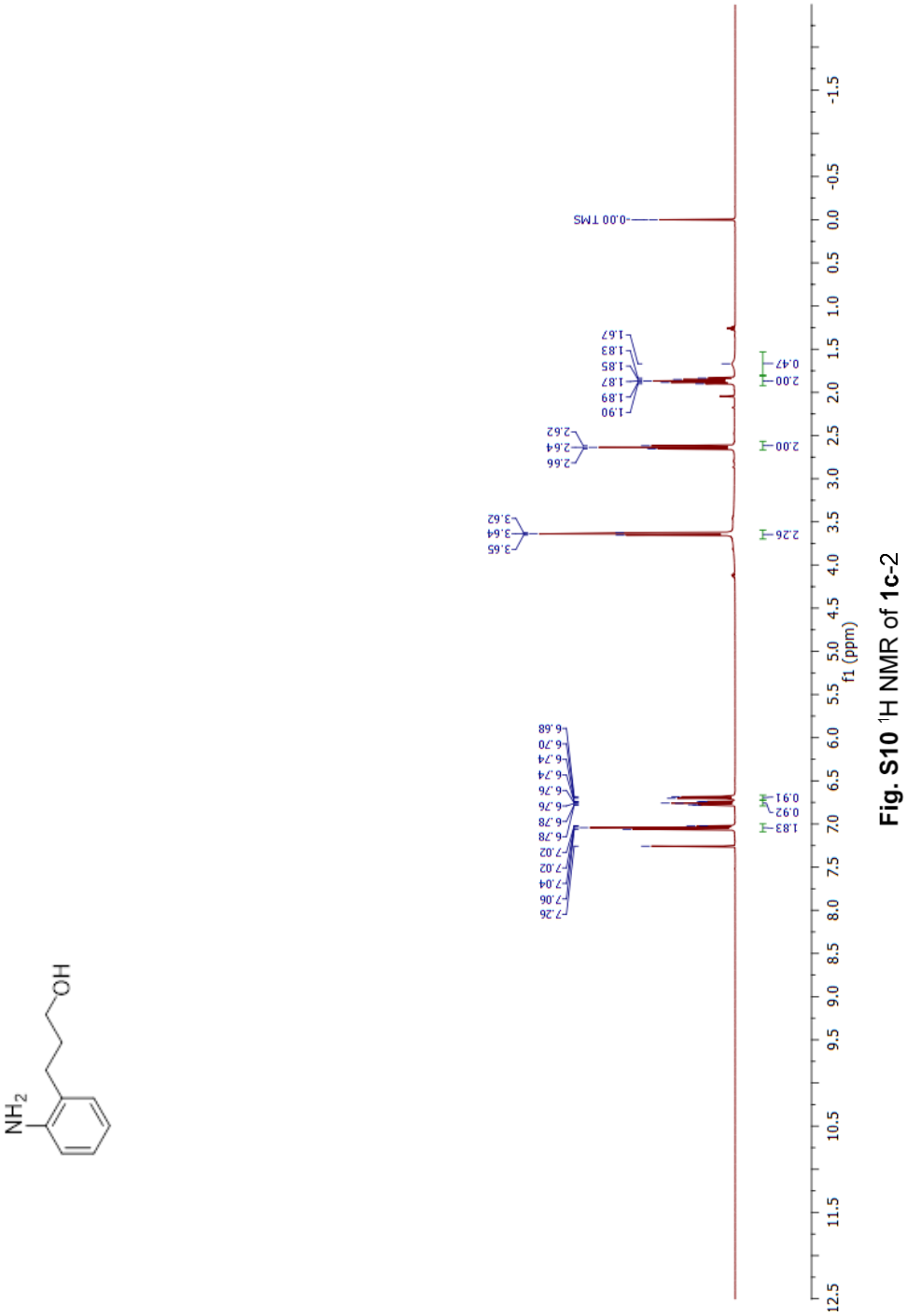

Fig. S10 ^{1}H NMR of **1c**-2

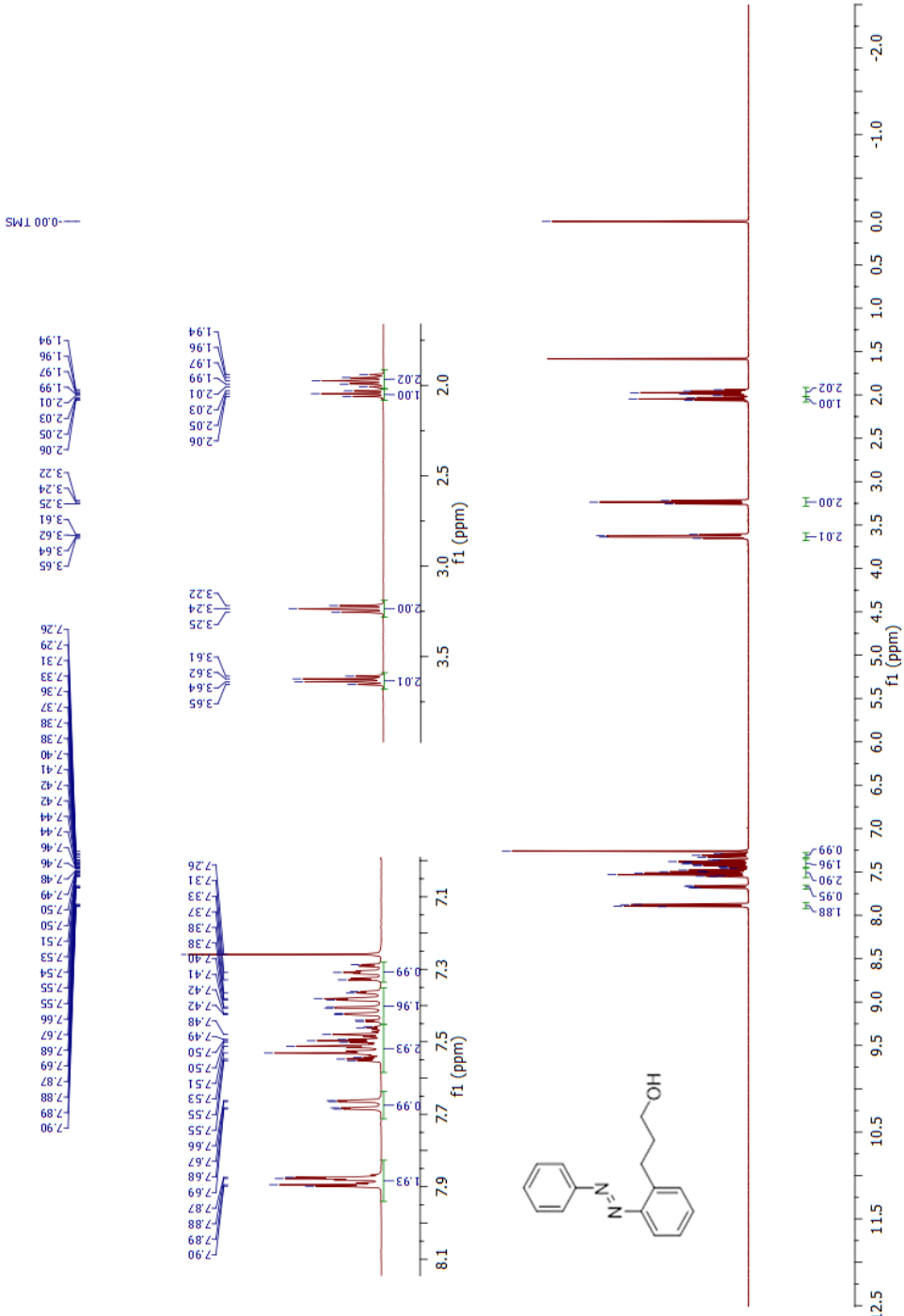

Fig. S11 ^{1}H NMR of **1c**-3

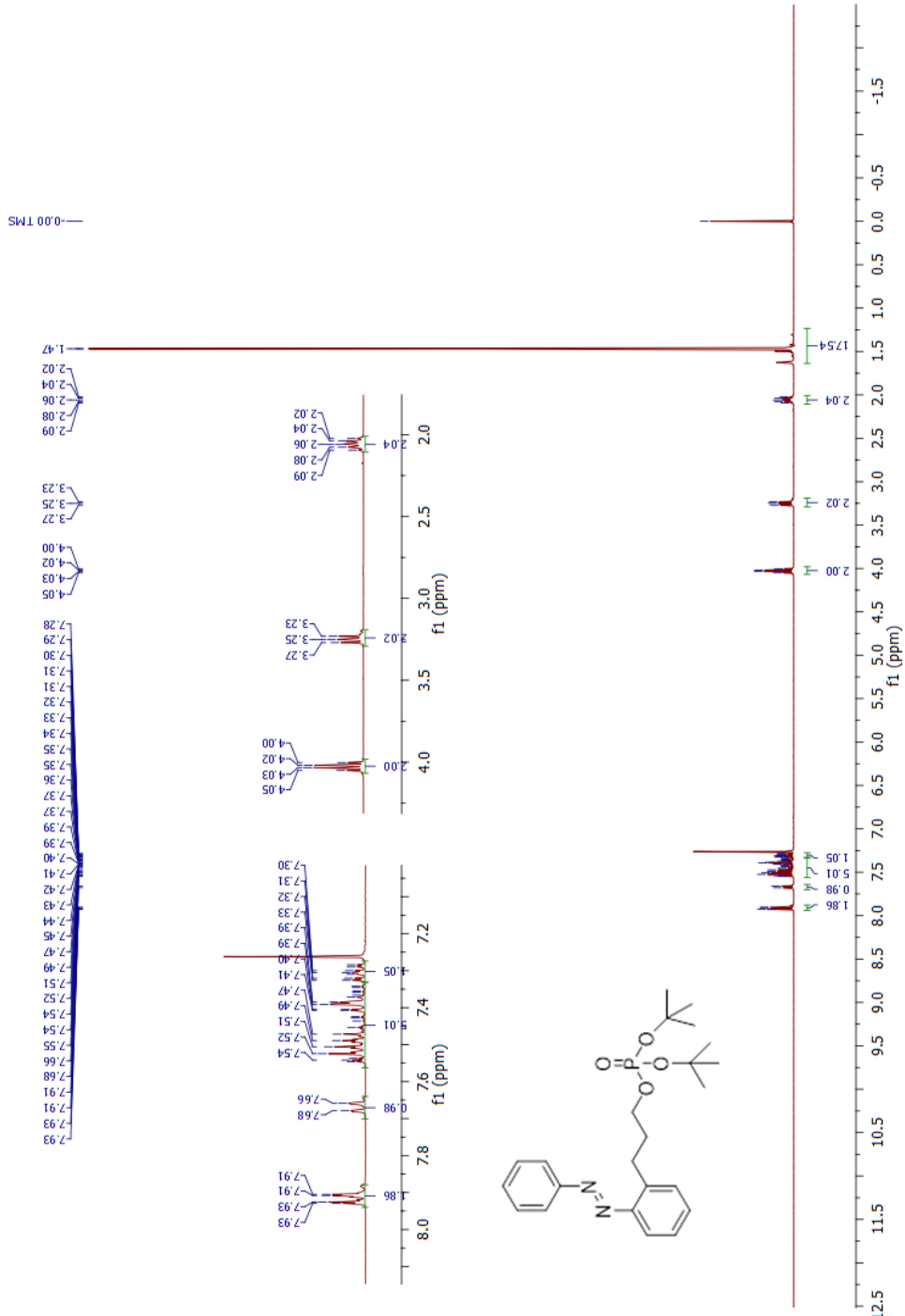

Fig. S12 ^{1}H NMR of **1c**-4

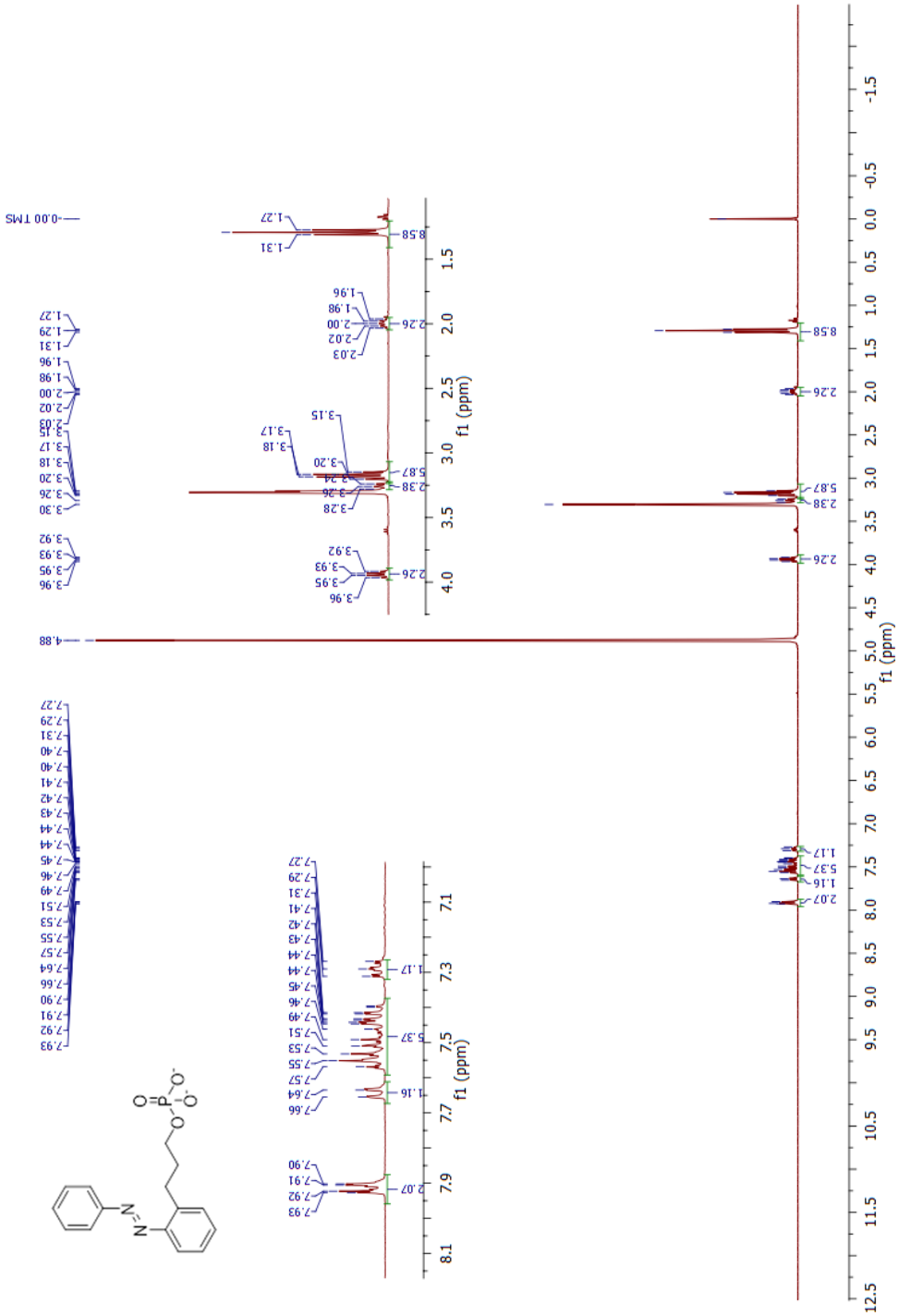

Fig. S13 ^{1}H NMR of **1c-5**

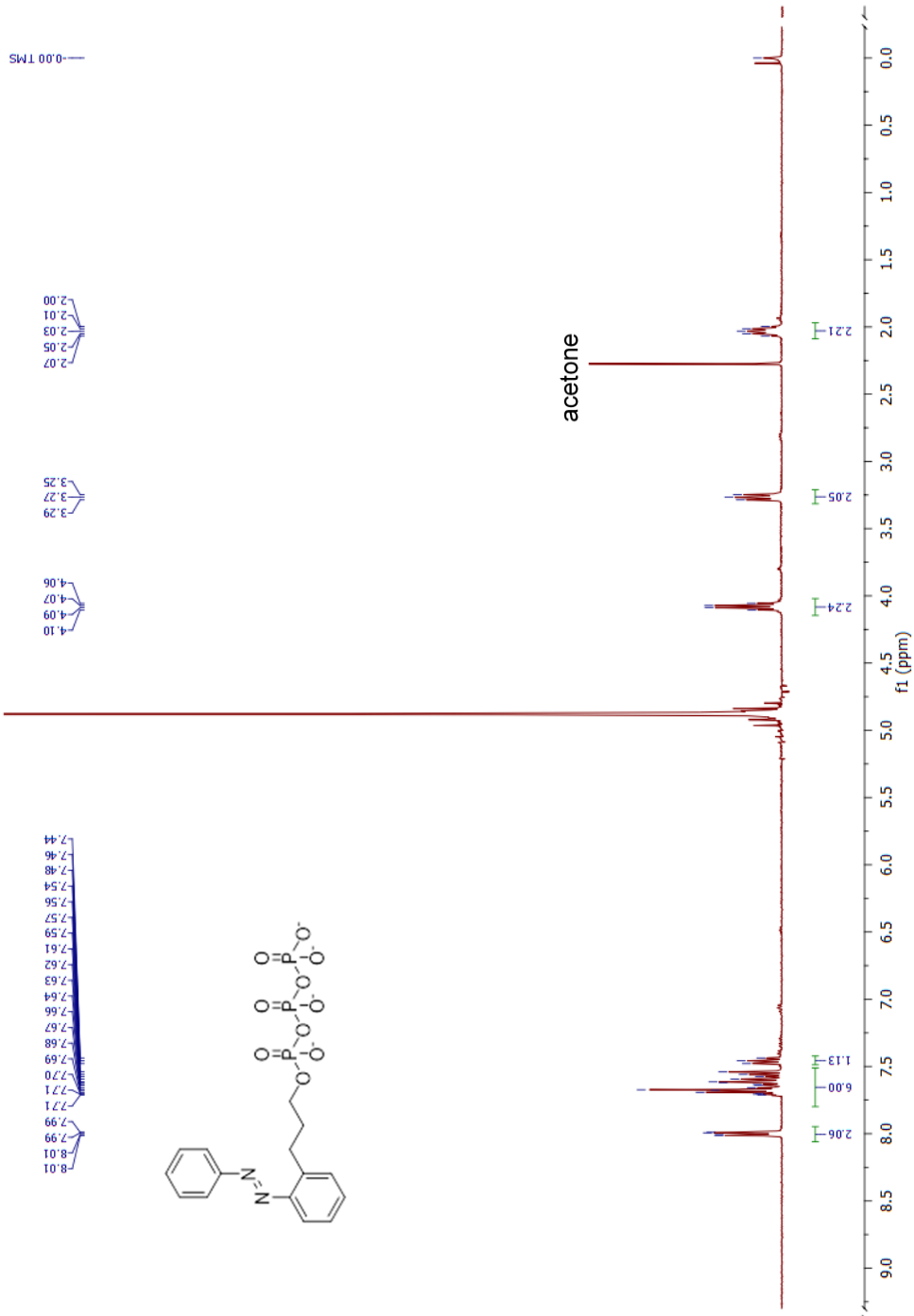

Fig. S14 ^{1}H NMR of **1c**

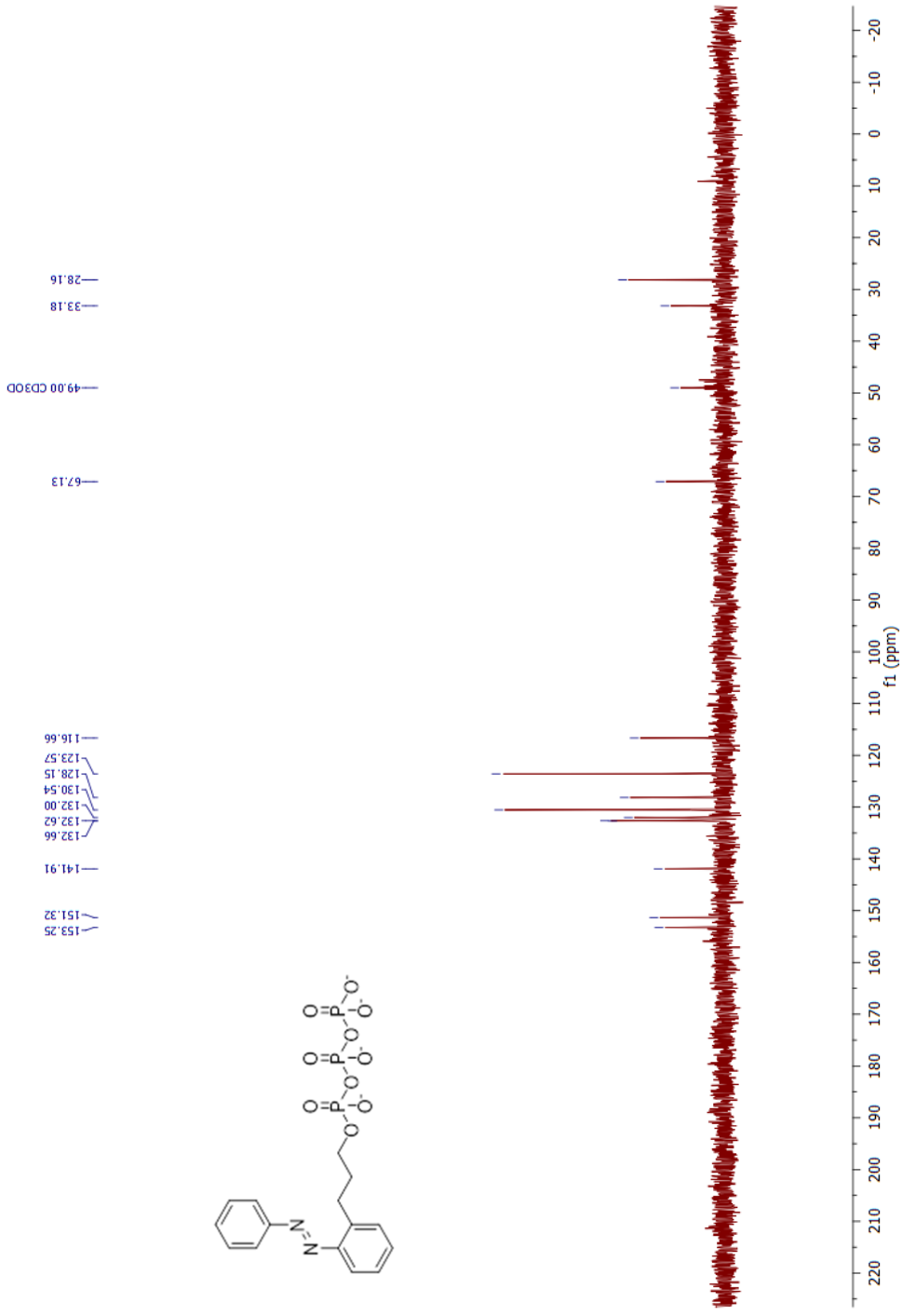

Fig. S15 ^{13}C NMR of **1c**

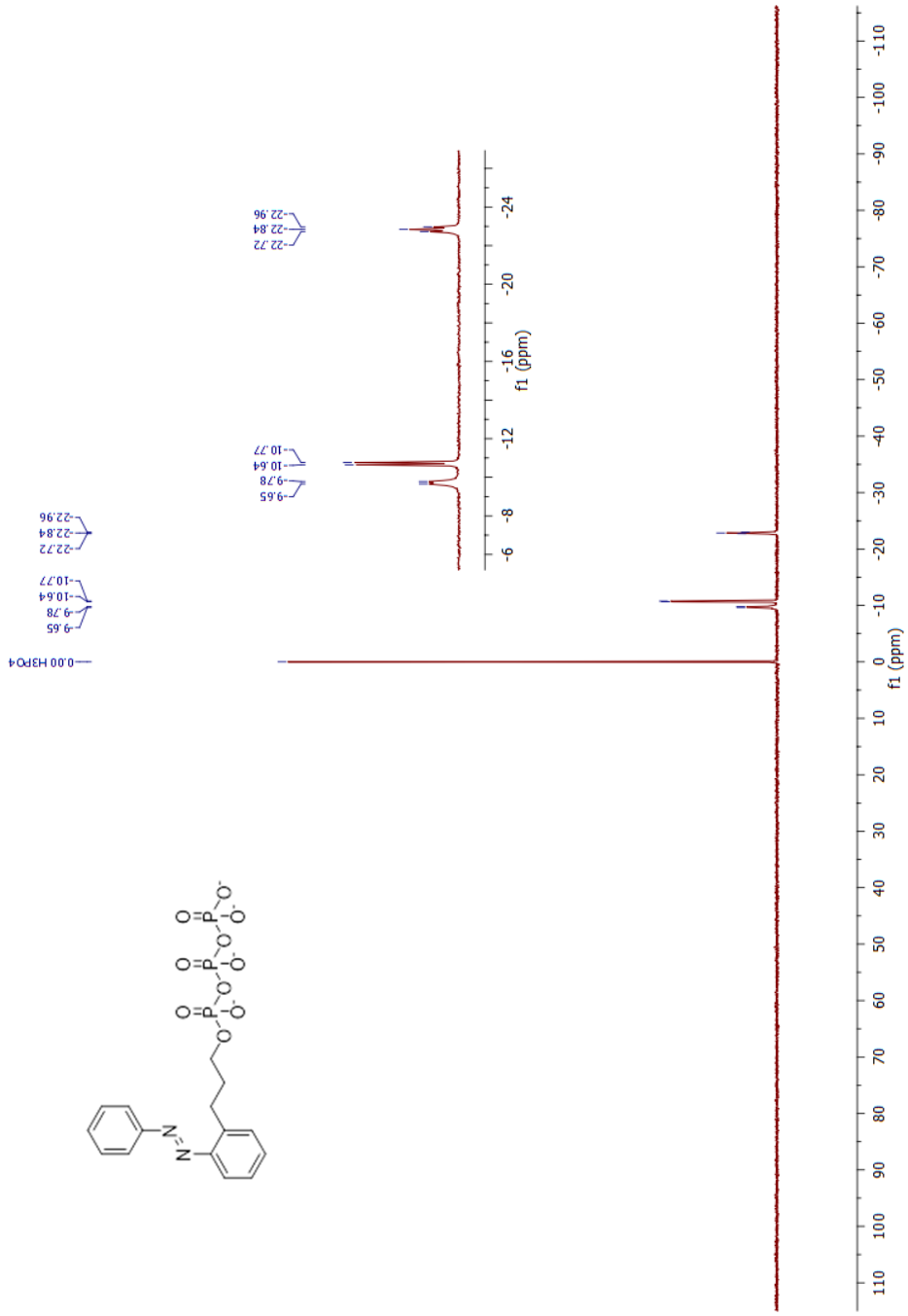

Fig. S16 ^{31}P NMR of **1c**

12. High-resolution mass spectra data of 1c

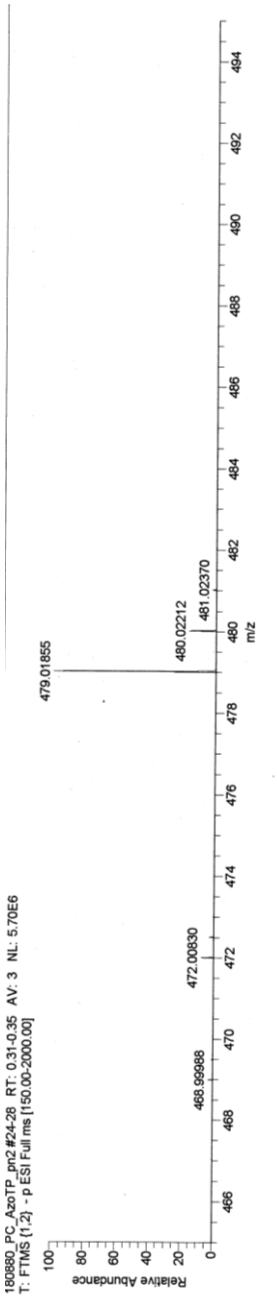

Fig. S17 High-resolution mass spectrum of **1c.** Calculated MS for $C_{15}H_{19}N_2O_{10}P_3$ $[M - H]^-$: 479.01798

References

1 N. Perur, M. Yahara, T. Kamei and N. Tamaoki, *Chem. Commun.*, 2013, **49**, 9935–9937.

2 H. M. Menezes, M. J. Islam, M. Takahashi and N. Tamaoki, *Org. Biomol. Chem.*, 2017, **15**, 8894–8903.